THE ASTROPHYSICAL JOURNAL, 271:175–182, 1983 August 1

THE SPATIAL DISTRIBUTION OF SHOCKED GAS IN THE ORION NEBULA

S. C. BECK[1] AND S. BECKWITH[1,2]
Department of Astronomy, Cornell University
Received 1982 November 8; accepted 1983 January 21

ABSTRACT

This paper presents observations of the spatial distribution of extinction and excitation temperature toward the molecular hydrogen emission in the Orion molecular cloud OMC-1. Most, although not all, of the observed structure in the near-infrared line intensities results from variations in the column density of vibrationally excited H_2 and is not due to variable extinction or temperature. The extinction toward the center of the emission region is between 1 and 2 mag at 4712 cm^{-1}, the frequency of the $v = 1$–0 $S(1)$ line, but increases toward the edges. The lack of emission from the eastern part of the nebula may result from increased extinction in that direction. Variations in the extinction temperature are less than the observational uncertainties of ± 200 K at all but one position observed. Therefore, the excitation temperature of the hydrogen molecules is probably not a strong function of either the shock velocity or the density of the gas. Observations of the $v = 3$–2 $S(3)$ line in the direction of strongest emission indicate the presence of gas temperatures about 2700 K and place constraints on the column density of gas which is at higher temperature.

Subject headings: interstellar: molecules — nebulae: Orion Nebula — shock waves

I. INTRODUCTION

Many stars undergo phases of violent mass loss during the last stages of their formation. The energy and momentum of these outflows is in some cases sufficient to alter the environment and dynamics of the cloud in which the star is formed and may well govern the rate of subsequent star formation (Norman and Silk 1980; Bally and Lada 1983). Broad molecular emission lines are observed close to the sources of expansion, and evidence for shocked molecules can frequently be seen where outflowing matter from the star accelerates material in the surrounding cloud. Emission from molecular hydrogen is one of the best tracers of the shocked gas where the outflow interacts with the cloud.

The brightest and best studied object exhibiting mass outflow and H_2 emission is the Orion molecular cloud (OMC-1). The H_2 emission is mainly confined to two lobes of unequal size and brightness which lie on opposite sides of the Kleinmann-Low Nebula (KL), and may be correlated with two oppositely directed expanding jets recently discovered very close to the cluster of stars in KL (Erickson *et al.* 1982). When observed with high spatial resolution, the H_2 emission consists of several small peaks of intensity on an extended background (Beckwith *et al.* 1978). The significance of the peaks is not clear; one suggestion is that some of the structure may be due to a source, not in KL, concurrently (or in the recent past) undergoing mass loss (Beck 1981).

The foreground extinction is sufficiently large that slight spatial variations in the extinction can change the apparent distribution of line intensities. Variations in the H_2 excitation temperature also affect the intensity distribution. Observations of the extinction toward one bright peak indicate much of the apparent intensity structure is produced by structure in the extinction (Scoville *et al.* 1982), but these observations cover only a limited part of the nebula.

In this paper, we examine the extent to which variations in extinction and excitation temperature govern the appearance of the H_2 brightness. We present new observations which extend previous work on the subject in three ways: First, extinction is derived from two lines whose intensity ratio should be more sensitive to the effects of extinction than those used earlier; second, the excitation temperature is observed almost simultaneously with the extinction to determine the effects of excitation temperature on the line intensities; and third, the spatial coverage of these observations is greater than previously obtained. Additionally, variation in excitation temperature with vibrational level of the molecules is studied by measurements of lines from three different vibrational levels. Section II describes the observations of H_2 line fluxes. Section III presents the analysis used to interpret the line ratios; a discussion of the results is given in § IV, and in § V we discuss what these measurements reveal about the structure of OMC. Many of the assumptions used in the analysis are discussed in a previous paper (Beckwith *et al.* 1983), to which we refer the reader for more detail.

II. OBSERVATIONS

The observations were made on the 3 m Infrared Telescope Facility (IRTF) at Mauna Kea with the cooled

[1] Guest Observer at the Infrared Telescope Facility, which is operated by the University of Hawaii under contract to the National Aeronautics and Space Administration.
[2] Alfred P. Sloan Foundation Fellow.

TABLE 1

H_2 LINE FLUXES, FOREGROUND EXTINCTION, AND EXCITATION TEMPERATURE IN THE ORION MOLECULAR CLOUD

POSITIONS (referred to Peak 1)	BEAM	CORRECTION	1–0 $S(1)$ FLUX ($\times 10^{-13}$ ergs s^{-1} cm^{-2})	1–0 $Q(3)$ FLUX ($\times 10^{-13}$ ergs s^{-1} cm^{-2})	2–1 $S(1)$ FLUX ($\times 10^{-13}$ ergs s^{-1} cm^{-2})	1–0 $S(2)$ FLUX ($\times 10^{-13}$ ergs s^{-1} cm^{-2})	0–0 $S(8)$ FLUX ($\times 10^{-13}$ ergs s^{-1} cm^{-2})	EXTERNAL $A_{2.122\,\mu m}$ (mag, ± 0.33 mag)	T_{vib} (K, ± 200 K)	OTHER LINES ($\times 10^{-13}$ ergs s^{-1} cm^{-2})	
										2–1 $S(3)$	3–2 $S(3)$
Pk 1	8″	1.5	47.5 ± 0.2	40.9 ± 0.6	5.0 ± 0.8	16.1 ± 0.6	31 ± 2	1.4	2050	3.1 ± 0.2	0.74 ± 0.15
8″S, 8″W	8″	1.2	65.2 ± 0.5	54.2 ± 0.5	5.9 ± 0.4	23.8 ± 0.8	33 ± 4	1.3	1970	...	...
16″S, 16″W	8″	1.0	23.9 ± 0.6	21.9 ± 0.4	3.1 ± 0.6	7.6 ± 0.7	18 ± 4	2.2	2200	...	...
8″N, 8″E	8″	1.3	31.8 ± 0.3	28.8 ± 0.7	3.0 ± 0.6	10.4 ± 0.6	32 ± 5	2.2	1930	...	...
IRc2	8″	1.5	39.2 ± 0.7	30.2 ± 0.8	1.9 ± 0.5	13.0 ± 0.3	23 ± 3	1.3	1600	...	...
8″N, 16″E	8″	1.0	11.2 ± 0.8	9.8 ± 0.4	0.7 ± 0.5	3.0 ± 0.8	14 ± 2	3.0	1690	...	...
24″S	8″	1.4	26.7 ± 0.5	...	3.6 ± 0.4	10.1 ± 0.6	17 ± 3[a]	1.3	2270	...	...
24″S, 8″W	8″	1.1	14.2 ± 0.3	...	1.4 ± 0.2	4.9 ± 0.7	...	3.0[b]	1910	...	...
24″W	8″	1.0	28.3 ± 0.7	...	2.3 ± 0.5	10.7 ± 0.7	21 ± 2[a]	1.9	1860	...	...
12″S, 12″E	8″	1.4	26.8 ± 1.0	...	4.4 ± 0.7	5.9 ± 0.8	16 ± 2[a]	1.9	2400	...	...
30″S, 30″E	8″	1.0	36.9 ± 0.9	...	3.2 ± 0.4	13.0 ± 0.8	17 ± 2[a]	1.4	1940	...	...
30″S, 18″E	8″	1.5	22.9 ± 0.7	...	1.7 ± 0.5	8.6 ± 0.9	14 ± 2[a]	1.2	1820	...	...
6″N, 6″E	6″	1.3	...	...	...	10.5 ± 0.9	28 ± 2[a]	2.0	...	...	...
6″N, 6″W	6″	1.0	...	...	...	23.2 ± 0.7	38 ± 2[a]	1.7	...	...	...
6″S, 6″E	6″	1.5	...	...	...	8.2 ± 0.5	20 ± 3[a]	1.7	...	...	...
6″S, 6″W	6″	1.2	...	...	...	17.0 ± 0.7	31 ± 3	1.6	...	...	...
12″S, 12″W	6″	1.15	...	...	...	9.5 ± 0.7	12 ± 2	1.2	...	...	...
24″S, 12″W	6″	1.1	...	...	...	1.6 ± 0.8	11 ± 3	3.4 ± 0.5[c]	...	...	...
24″S, 12″E	6″	1.5	...	...	...	5.4 ± 0.7	14 ± 3	1.8	...	...	...
18″S, 18″W	6″	1.0	...	...	...	5.2 ± 0.7	19 ± 3	2.7	...	...	...
18″S, 12″E	6″	1.3	...	...	...	3.2 ± 0.7	9 ± 1	2.0	...	...	...
24″S, 36″E	6″	1.0	...	...	...	3.7 ± 0.7	6 ± 2	1.7 ± 0.4[c]	...	...	...
36″S, 36″E	6″	1.0	...	...	...	3.7 ± 0.8	3 ± 1.5	0.9	...	...	...
24″S, 24″E	6″	1.0	...	...	...	12.1 ± 0.7	24 ± 3	1.9	...	...	...
36″S, 24″E	6″	1.0	...	...	...	5.9 ± 0.7	9 ± 2	1.6	...	...	...

NOTE.—The fluxes listed are those observed uncorrected for internal or external extinction. The extinctions listed have the correction factor already included; i.e., the 1–0 $S(2)$ flux in the extinction calculation equals that in the table times correction. T_{vib} was calculated after correcting the line fluxes for extinction.

[a] In these positions the 1–0 $S(2)$ and 0–0 $S(8)$ measurements were made with a 6″ beam.

[b] No $S(8)$ measurement; extinction estimated from other lines and therefore more uncertain (± 0.7 mag).

[c] In these two positions the formal errors in the extinction are very large and are shown explicitly. The large errors are due to the weakness of the lines; in neither position were both lines detected at the 3 σ level.

grating spectrometer described by Beckwith *et al.* (1983). The observations were made in two parts. The first were carried out in 1981 November using a 6″ diameter beam. The $v = 1$–$0\ S(2)$ and $v = 0$–$0\ S(8)\ H_2$ lines were observed at 19 positions in OMC-1 (those mentioned in Table 1 plus Peak 1). The telescope was offset from θ^1 Orionis C to each position; θ^1 Orionis C was observed at least once every 10 minutes to make small pointing corrections. The positions are accurate to 0.″5 ($\pm 1\ \sigma$). The sky background was cancelled by chopping 60″ in right ascension. These observations form the basis for most of the extinction analysis described in the next section.

Additional observations were made in 1982 January and February. An 8″ diameter beam was used for these measurements, but the pointing, chopping, and observing technique were identical to those used in 1981 November. The $v = 0$–$0\ S(8)$, $v = 1$–$0\ S(1)$, $S(2)$, $Q(3)$, $v = 2$–$1\ S(1)$ lines were observed at 12 positions including six positions which were also observed in 1981 November. Figure 1 shows the positions corresponding to the different measurements. At the position called Pk 1 by Beckwith *et al.* (1978), we measured the $v = 3$–$2\ S(3)$ and $v = 2$–$1\ S(3)$ lines together with all the lines mentioned above.

The line strengths were measured by sampling seven wavelengths spaced by one-half the instrumental resolution centered on each line. The instrumental resolution was between 600 and 1000 ($\lambda/\Delta\lambda$), which was sufficient to isolate each line but not to resolve individual lines, so fluxes were determined by fitting the instrumental profile to the data. The uncertainties shown in Table 1 are formal uncertainties from the line-fitting procedure. There is an additional overall uncertainty in the flux density scale of about 10%. The flux density scale was calibrated by observations of the bright stars 1948 and 1941; we assumed magnitudes of 2.31 and 3.68 at 2.12 μm for these stars, respectively.

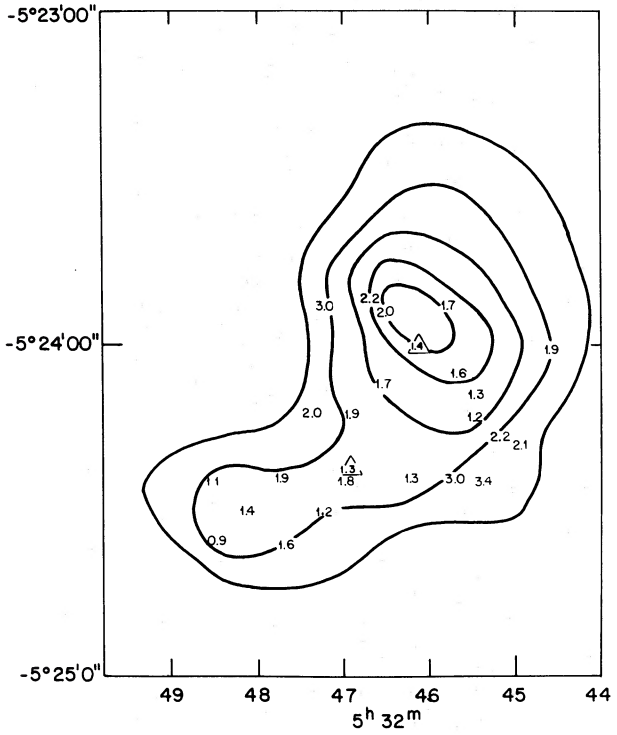

FIG. 1.—The external extinction at 4712 cm^{-1} (2.12 μm) in magnitudes is displayed superposed on the intensity contours of $v = 1$–$0\ S(1)$ emission. The intensity map is from Beckwith *et al.* (1978) and has 13″ resolution. The beam sizes of the extinction measurement may be found from the table. The northern triangle marks Pk 1, and the southern, IRc2.

The frequency scale was measured in the laboratory by observations of argon and krypton lines with well-known frequencies; at the telescope, frequencies were determined from the positions of telluric absorption features and, for strong lines with well-known frequencies, from the positions of the H_2 lines themselves. From the constants of Beck, Lacy, and Geballe (1979), we calculated the $v = 0$–$0\ S(8)$ line to be at 1980.24 cm^{-1} or 5.0499 μm; the line was observed to be at 1979.8 ± 0.4 cm^{-1}, in good agreement with the calculated frequency and with the observations of Knacke and Young (1981). The constants of Bragg, Brault, and Smith (1982) give a frequency of 4542.56 cm^{-1}, or 2.2014 μm, for the $v = 3$–$2\ S(3)$ line; our observations indicate a frequency of 4542.0 ± 2 cm^{-1} for this line. The observed line is very weak, and the uncertainty in the line frequency is difficult to establish. In view of the small flux of the line, the detection should be considered tentative pending confirmation. The frequencies for the other lines presented in this paper are well known (Shull and Beckwith 1982).

The observations were made at Mauna Kea specifically to reduce interference by telluric water vapor. The 1–0 $S(2)$ line frequency is not close to any strong atmospheric absorptions that would distort the measured line flux, and this was borne out by the appearance of the standard-star spectra. The 0–0 $S(8)$ line is within 0.75 cm^{-1} of a narrow H_2O absorption, but again, the calibration spectra indicated that the effect of the line was a smaller source of error than other uncertainties in the measurements. The 1–0 $Q(3)$ line is close to a wide H_2O absorption feature, and as Scoville *et al.* show, the broad lines in the OMC can be heavily affected by the atmosphere even at a dry site. It is difficult to give a numerical estimate of the error associated with the atmospheric absorption since it depends on the air mass and the intrinsic width of the lines, but it should be noted that the 1–0 $Q(3)$ fluxes have a much higher uncertainty than the other lines by probably a factor of 2.

III. ANALYSIS

The line ratios can be used to determine the extinction and temperature of the molecules as follows: If the molecular levels are in thermal equilibrium at temperature T, the flux ratio of two lines, F_1/F_2, is

$$\frac{F_1}{F_2} = \frac{R_1 v_1 g_1}{R_2 v_2 g_2} \exp\left(-\frac{E_1 - E_2}{kT}\right) 10^{-(A_1 - A_2)/2.5}, \quad (1)$$

where R is the spontaneous emission rate; v, the photon frequency; g, the statistical weight of the upper state; E, the energy of the upper state; and A, the extinction

at frequency v (cf. Shull and Beckwith 1982). Only the exponential factors depend on conditions in the emission region through the temperature and the extinction. If either the temperature or the extinction is known, a measurement of the flux ratio from appropriate lines may be used with equation (1) to find the other quantity.

It can be seen from equation (1) that a line ratio will be most sensitive to extinction if $A_1 - A_2$ is large for large A_1; since $A_1 - A_2$ is a measure of the reddening between frequencies, the line frequencies should be well separated. In this case, the effects of temperature will be minimized if $E_1 \sim E_2$. Similarly, if two line frequencies are nearly the same, but $E_1 \gg E_2$, the line ratio will be most sensitive to the level temperature T. These principles dictated the choice of lines used to derive extinction and temperature as described in this section.

To determine the extinction, we used the ratio of the $v = 0$–0 $S(8)$ and $v = 1$–0 $S(2)$ lines, referred to with subscripts 1 and 2, respectively. For this line pair, $v_2 \sim 2.5v_1$, but $E_2 \sim 0.9E_1$, so changes in extinction affect the line ratio much more strongly than changes in temperature (actually, this statement depends on the coefficient $1/kT$, but the statement is true for the temperatures observed in OMC-1). Assuming a temperature of 1700 ± 200 K (discussed below) and using the emission rates calculated by Turner, Kirby-Docken, and Dalgarno (1977), the line ratio depends on the extinction as

$$F_1/F_2 = (0.4 \pm 0.03)10^{(A_2 - A_1)/2.5}, \qquad (2)$$

subscripts 1 and 2 referring to the $v = 0$–0 $S(8)$ and $v = 1$–0 $S(2)$ lines. If there were no uncertainty in F_1/F_2, the uncertainty in $A_2 - A_1$ would be 0.1 mag. Equation (2) is true if the extinction occurs entirely outside the region where the lines are produced.

If the lines are produced in an extended region along the line of sight and extinction occurs within as well as outside the region of line emission, equation (2) will not be true, and the ratio of two lines will depend on the distribution of line intensities and extinction throughout the region of emission. This is the case for the H_2 emission in OMC-1. The H_2 lines are produced in a differentially expanding volume at velocities of more than 100 km s^{-1} with respect to the center of momentum velocity (Nadeau, Geballe, and Neugebauer 1982, hereafter NGN; Scoville *et al.* 1982; Beck *et al.* 1982). The spectra show that the low-frequency sides of the lines are weaker than the high-frequency sides of the lines, presumably because the gas expanding away from us is affected by extinction within the expanding volume.

The line shapes can be used to correct for extinction within the emission region by the following method: We assume that the 1980 cm^{-1} lines are intrinsically symmetric and are not affected by extinction within the expanding volume at all, and that the high-frequency sides of the 4919 cm^{-1} lines are also free of distortion. We justify these assumptions by noting (1) the high-velocity motions in Orion as shown by ^{12}CO lines have extremely symmetric velocity profiles, (2) the 814 cm^{-1} $v = 0$–0 $S(2)$ lines measured by Beck *et al.* (1982), which have the same susceptibility to internal obscuration as do the 1980 cm^{-1} lines, are symmetric except in a few positions which the current map did not cover (and in which the line asymmetry is not due to internal extinction but to discrete velocity components), and (3) the high-frequency sides of the 2 μm lines observed by NGN and Scoville *et al.* are only slightly affected by obscuration, and although the line centers can be shifted measurably by internal extinction, the total flux of the high-frequency sides is not reduced by more than a few percent.

If the high-frequency sides of the lines could be isolated and compared, the line ratios should indicate the extinction in front of the emission region. Since the lines are unresolved in the present experiment, we examined instead the spectra of NGN on or as close as possible to each observed position and determined what fraction of the line flux is contributed by the high-frequency side. We then multiplied the observed line fluxes by twice this factor (the "correction" listed in Table 1) to give a line flux equal to twice the high-frequency side flux. The correction ranges from 1, for no internal extinction, at the edges of the emitting region to 1.5 (meaning that one-third the line flux is obscured inside the emitting region) at the center. After the 4919 cm^{-1} lines are so corrected, a ratio of one-half the 1980 cm^{-1} to one-half the 4919 cm^{-1} fluxes should compare the blue sides accurately and result in a measurement of only foreground extinction. Throughout this paper we shall refer to *internal* extinction as that due to absorbing material inside the emitting region, which we have just removed from our calculations, and to the extinction due to material between the emission region and the observer as *foreground* and *external*. The structure observed in the absence of foreground extinction will be referred to as intrinsic; the *intrinsic* structure may still be affected by internal extinction.

If F_1 is also affected by extinction within the emission region, the foreground extinctions given in Table 1 are underestimates. Velocity-resolved profiles of the 0–0 $S(8)$ line at v_1 are not available, but velocity profiles of the $v = 0$–0 $S(2)$ line are. The extinction at v_1 should be about the same as that at the $v = 0$–0 $S(2)$ frequency, 814 cm^{-1}, assuming a standard reddening curve (Johnson 1968) with silicate absorption. The 0–0 $S(2)$ lines show no evidence of internal obscuration except toward IRc2 (Beck 1981).

The correction method we have adopted will also break down if the internal obscuration is so extreme that the centers and high-frequency sides of the lines are obscured. On IRc2, for example, the internal extinction is so severe that the apparent peak of the 4919 cm^{-1} emission is blueshifted 50 km s^{-1} from that of the 814 cm^{-1} emission. In this case even doubling the observed 4919 cm^{-1} emission (which is the maximum possible correction factor) will be an undercorrection, and the foreground extinction will be overestimated. Such severe obscuration is unlikely to affect any of the results shown in Table 1 with the possible exception of that toward IRc2 itself.

Following standard practice, we refer the total extinction, denoted A_0, to the frequency of the well-mapped $v = 1$–0 $S(1)$ line at 4712 cm^{-1}. The reddening law is assumed to follow curve #15 of van de Hulst extrapolated to the infrared region (Johnson 1968) in which $A(\nu) \sim \nu^{1.9}$, and this law is used to derive A_0 from $A_1 - A_2$. Different investigators find the reddening law to range from $A(\nu) \sim \nu$ to $A(\nu) \sim \nu^{2.5}$ in various dark clouds, and the exponent 1.9 is not well established for Orion. Because the two lines used to find the reddening differ by a factor of 2.5 in frequency, however, the relative extinction between ν_1 and ν_2 is nearly the same as the total extinction at ν_2, and the derived extinction A_0 is relatively insensitive to the uncertainty in the extinction law. Using the two extremes of the range quoted here changes A_0 by a factor of about 1.5.

The excitation temperature used in the extinction analysis is intermediate between 1500 K, which characterizes levels with $E/k \sim 7000$ K, and 2000 K, which characterizes levels with $E/k \sim 12{,}000$ K, since the upper levels for the two lines under discussion have $E/k \sim 9000$ K. The uncertainty was chosen mainly to reflect the possible error in assuming constant temperature in different locations in the nebula, but it might also reflect the possible error in the assumed excitation temperature appropriate for these particular levels.

To determine the excitation temperature, we used the ratio of the $v = 2$–1 $S(1)$ and $v = 1$–0 $S(1)$ lines, referred to with subscripts 3 and 4, respectively. In this case, $\nu_3 \sim \nu_4$, and $E_3 \sim 1.8E_4$, so the line ratio is almost independent of extinction but is a strong function of temperature. Equation (1) was used with the appropriate molecular constants to determine T at each point where these two lines were measured. Beckwith *et al.* (1983) pointed out that excitation temperature varies with the level energy of the lines measured. We extended this result by measuring lines from three different vibrational levels in the direction of Pk 1 and determining the vibrational temperature in levels up to $v = 3$. This is the first detection of a line from the $v = 3$ state.

IV. RESULTS

Table 1 shows the observed fluxes of the H_2 lines along with the extinction and temperature at each position calculated as described in the last section. Column 3 lists the correction factors applied to the $v = 1$–0 $S(2)$ line to account for extinction within the region of line production. Two of the lines, the $v = 1$–0 $S(2)$ and $v = 0$–0 $S(8)$ lines, were observed at the same six positions in 1981 November and 1982 February, and the separate measurements agree quite well when the different beam sizes are taken into account. The uncertainties listed in the table for the derived extinction (± 0.33 mag) and temperature (± 200 K) account for both the statistical and observational uncertainties but do not reflect possible systematic uncertainties associated with the assumptions made to analyze the data.

The H_2 fluxes measured repeated well from night to night and from November to February runs. The observed fluxes agreed fairly well, when adjusted for the different apertures used, with previous measurements of the same lines, with two exceptions. The $S(9)$ line mapped by Knacke and Young (1981) should have the same distribution as the $S(8)$ transition, but it shows a peak south of the BN object where the $S(8)$ emission is weak. The $S(9)$ feature is not seen in the $S(2)$ intensity distribution either, and we believe the discrepancy may be due to small differences in pointing. The $S(8)$ line flux we measure on Peak 1 is almost 3 times less than that Knacke and Young (1981) report. We do not understand the cause of this disagreement, although it may in part be due to the fact that the two groups used different calibrations. We have used the lower flux measurement in this paper because of the consistency and reproducibility of our calibrations and because it fits very well in the expected intensity versus energy level relation using lines presented here in addition to lines measured by Beckwith *et al.* (1983) at 5.5 and 6.9 μm.

Figure 1 shows the extinction derived at each of the observed positions on the map of $v = 1$–0 $S(1)$ line intensity made by Beckwith *et al.* (1978). The extinction varies from about 1.2 mag to 3 mag over most of the nebula. The extinction is smallest close to Pk 1 and Pk 2 and is largest at the edges of the map, particularly the eastern edge, where the contours fall off most rapidly. Although there is some anticorrelation of extinction with intensity (in that smaller intensity goes with larger extinction) in isolated areas, the general appearance of the map is not governed by variable extinction. Figure 2 is a plot of $v = 1$–0 $S(2)$ line intensity versus extinc-

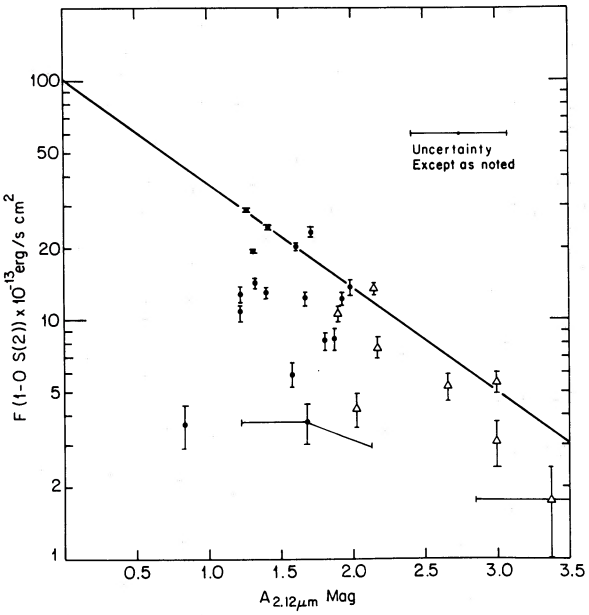

FIG. 2.—External $A_{2.12\,\mu m}$ in magnitudes vs. the uncorrected intensity of the 1–0 $S(2)$ line. The errors in $A_{2.12\,\mu m}$ are shown for the two positions with anomalously large uncertainties; the uncertainty in all other positions is shown at top right. The triangles are those positions at the edge of the nebula where the extinction increases most obviously. The diagonal line is where points would fall if the intensity were that of Pk 1 and only the extinction varied.

tion for 25 observed positions. As seen in the figure there is substantial variation in the actual line intensity.

The extinctions found here agree very well with those found by Scoville *et al.* (1982) in those positions observed by both groups. Some of the structure apparent in the 5″ resolution map of the Pk 1 area (cf. Beckwith *et al.* 1978) is the result of extinction variations as found by Scoville *et al.* (1982), but there are also places where the intensity decreases markedly with no obvious increase in the extinction, such as the center of the map near the infrared cluster. The present results probably agree with the extinction of 2–2.5 mag found by Davis, Larson, and Smith (1982) and Beckwith *et al.* (1983), when corrections are made between the 6″ resolution of this study and the approximately 30″ resolution of the others. Since the extinction rises away from Pk 1, the extinction averaged over a large area will be higher than the extinction seen toward Pk 1 with high spatial resolution.

Most of the early measurements of the extinction to the H_2 emission used the reddening between $v = 1$–0 $Q(3)$ and $S(1)$ lines to find A_0 (Simon *et al.* 1979; Beckwith, Persson, and Neugebauer 1979; Scoville *et al.* 1982; Davis, Larson, and Smith 1982). These lines were measured at six positions shown in Table 1 along with the $v = 0$–0 $S(8)$ and $v = 1$–0 $S(2)$ lines to check the consistency of the present method with the earlier results. In every case, the extinction implied by the $v = 1$–0 $Q(3)$ and $S(1)$ lines agrees with that found using the lines with greater frequency separation, but the uncertainties in the former case are considerably larger. The large uncertainties resulted mainly from statistical uncertainties in our observations, which have a greater effect on A_0 because of the small frequency separation of the lines, but it is also more difficult to obtain accurate observations of the $Q(3)$ line when the line profile is unresolved because the telluric absorption is large (cf. Scoville *et al.* 1982).

The excitation temperature between the $v = 1$ and $v = 2$ levels averaged over 12 positions is 1970 K, in good agreement with the results of other studies. Of these 12 positions, only one has a temperature 2 standard deviations or more from the mean. With this exception, the data are consistent with uniform excitation across the nebula. This result justifies the assumption of constant temperature used to estimate the extinctions.

The $v = 3$–2 $S(3)$ line flux is approximately one-fourth the flux of the $v = 2$–1 $S(3)$ line. The apparent vibrational temperature between the second and third vibrational states is therefore 2700 ± 300 K, somewhat higher than that found for the first and second vibrational levels. This result is in keeping with the observation that the excitation temperature increases with level energy. It is useful to note that the $v = 3$–2 $S(3)$ line should be very sensitive to the presence of very hot gas ($T > 3000$ K), but the line ratios show no indication of this gas.

V. DISCUSSION

The apparent distribution of shocked H_2 in OMC-1 is shown in the contour map in Figure 1. Observations of many molecules at many wavelengths led to a model of OMC-1 which is dominated by molecular gas expanding from a center in the Kleinmann-Low Nebula at velocities ≥ 100 km s^{-1}. The distribution of H_2 does not fit this model in any immediately obvious way. The shocked H_2 is not spherically symmetric nor is it exactly centered on KL, but rather it is concentrated in two lobes north and south of KL, the northern of which is larger and brighter than the southern. The three features of the H_2 distribution which do not fit readily into the usual model of KL-centered gas flows and which could be due to foreground obscuration are the two lobes of unequal intensity, the region of low brightness on KL itself and the north-south elongation. These are discussed in turn below.

a) The Appearance of the H_2 *Distribution*

The H_2 emission is most intense in two regions; one $\sim 45''$ in diameter centered $\sim 20''$ NW of KL and the other $\sim 30''$ in diameter centered $\sim 15''$ SE of KL. The peak brightness of the southern region is approximately one-half that of the northern. The difference in foreground extinction to the two regions is not great enough to explain the intensity difference. There is no evidence for increased extinction at the southern end of the emission, which could account for that lobe's small separation from KL, nor for increased extinction at the edges, which could explain the small diameter. We can conclude that the H_2 emission in OMC-1 is asymmetric in intrinsic brightness, extent, and distance from the KL Nebula. Either the flow or the ambient cloud is different north and south of KL.

Since the gas outflows producing the shocked H_2 are believed to originate in the KL region, the weak H_2 line intensity in that area is an important factor in models of OMC-1. Observations on and near IRc2 show that A_0 is 1.3–1.7 mag, no greater than around Peak 1 and less than on the edges. The weakness of H_2 emission in the center of the map area is therefore not due to foreground extinction but results from a low column density of vibrationally excited H_2 in front of KL. It is possible that a large column density of excited H_2 exists behind KL with a very large intervening (internal in our nomenclature) extinction, but this possibility cannot be determined from our data.

Other observations of the KL region (Plambeck *et al.* 1982) found an extremely dense disk of material oriented roughly perpendicular to the H_2 lobes. The infrared point sources are on the near side of the disk. This disk could provide the extinction which we suggest may be responsible for the lack of observable H_2. If this disk does in fact constrain the outflow from KL, some feature of its structure may also be related to the differences in H_2 emission in the northern and southern lobes.

The extinction increases toward the edges of the northern emission region. The gradient appears in all directions except NW of Peak 1, and the extinction becomes greatest where the emission falls off fastest, NE and SW of the peak. The region of heavy obscuration extends at least 40″ along the western edge of the source.

The observed pattern might be produced in several

ways. Two extreme examples would be if the emission were intrinsically spherical and the foreground extinction came from some intervening cloud, independent of the OMC-1 system, or if the emission region were expanding into dense obscuring clouds which physically interfere with the expansion. Unfortunately, there is at this time no way of distinguishing between these cases.

b) *Correlation of Extinction with Other Traces of Dense Material*

Bastien *et al.* (1981) found evidence in the H_2CO observations for two large ($l \sim 0.1$ pc) dense [$n(H_2) > 10^6$ cm^{-3}] molecular clouds which are not involved in the violent motions of the KL region and whose positions are marked in Figure 3. The visual extinction through each cloud, estimated from radio observations, is ~ 100 mag. The clouds border the H_2 emission and Bastien *et al.* argue that they produce the elongated surface brightness by either of the extreme methods described above or some combination. However, the position of the clouds and the H_2 structure do not correlate in detail. The southern 8.0 km s^{-1} cloud lies at an edge of the H_2 emission where there is neither high extinction nor a strong gradient in the extinction. The northern 9.8 km s^{-1} cloud appears to overlap both a region of high H_2 extinction and the brightest and least obscured H_2 peak. Both of the clouds are barely resolved spatially by the radio observations, and spatial displacements of fractions of the radio beam sizes would change the degree of correlation with the H_2 intensity. But at present, the dense quiescent clouds do not seem to have a clear effect on the H_2 structure.

Plambeck *et al.* (1982) mapped SO, a molecule which preferentially traces regions of very high gas density, with 6″ resolution. They found SO emission centered within a few arc seconds of IRc2 and covering an area of 11″ × 19″, elongated NE-SE (see Fig. 3). The column density of gas derived from the SO observations implies a visual extinction of roughly 1000 mag at IRc2. This number does not in fact contradict our figure of $A_v \sim 15$ mag to the H_2 emission toward IRc2 or Downes *et al.*'s (1981) result of $A_v \sim 40$ mag from the silicate absorption on IRc2, because the three sets of observations probably measure very different depths along the line of sight. Plambeck *et al.* point out that the infrared point sources seen in this region must lie near the surface of the SO emission. The extinction we measure to the H_2 emission is as usual that in the foreground only. The weakness of the H_2 emission near the infrared cluster may be due in part to very dense internal obscuration, which blocks out more than just the blue sides of the 2 μm lines and causes the method we have used for correcting line fluxes to break down.

c) *The Near Uniformity of Temperature*

The above discussion has shown that there are significant intensity variations in the H_2 emission which are not due to extinction. It is interesting to compare

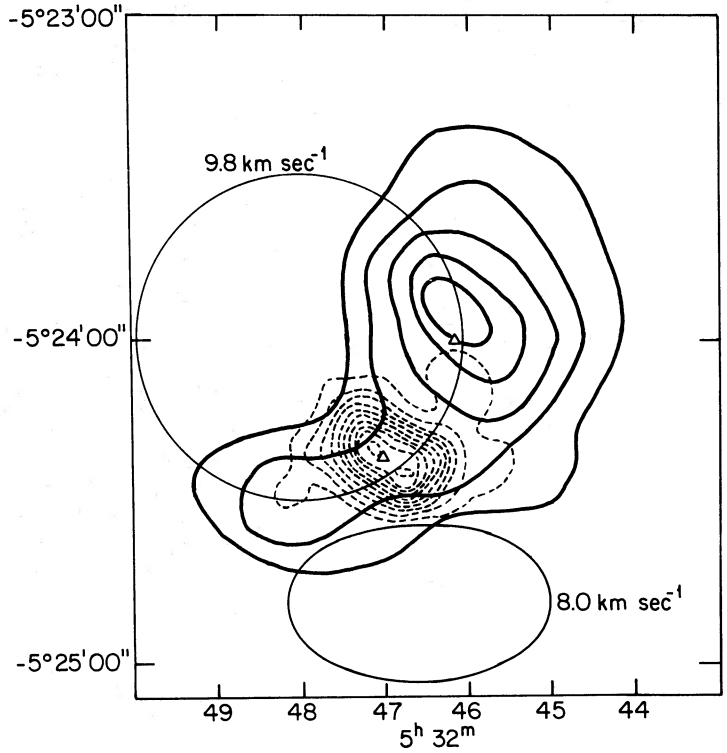

FIG. 3.—The location of dense clouds, displayed on the 1–0 $S(1)$ intensity contours. The clouds marked 9.8 and 8.0 km s^{-1} are those found by Bastien *et al.* (1981) and have $A_v \sim 100$ mag. The dotted lines are the intensity contours of SO 2_2–1_1, 86 GHz emission, mapped by Plambeck *et al.* (1982) with a 6″ beam. The visual extinction through that cloud is ~ 1000 mag.

the differences in intensity with the near uniformity of the H_2 gas temperature. The temperature of 1700 ± 200 K applies to the major portion of the nebula and to points of very different shock intensities. It is possible that there is some mechanism in postshock gas that tends to fix the temperature at a single value. The H_2 gas temperature in other sources, including evolved objects such as CRL 618, is also observed to be 2000 ± 500 K (Thronson 1981). It is perhaps easiest to explain the variations in intensity which are not correlated with variations in temperature by assuming that there is some thermostat in effect, and the intensities are determined by the density of the gas and the number of shocks which have heated the gas in the line of sight. In different beam positions, different fractions of the H_2 column may have been heated by shocks in the recent past. In this case the intensity variations would reflect differences in the structure and history of the outflow and the ambient medium, not necessarily in the gas density or the velocity of the exciting shock.

VI. SUMMARY AND CONCLUSIONS

We have mapped several H_2 emission lines in the Orion molecular cloud in an attempt to determine the structure in the temperature and extinction of the source. Our major conclusions are as follows:

1. The extinction in the central part of the cloud varies from 1.2 to 2.0 mag at 2.12 μm. It increases at the eastern and western edges to as much as 3.5 mag. The weakness and small extent of the emission south of KL compared with that in the north are not due to foreground obscuration but reflects intrinsic source properties. The weakness of H_2 toward the KL region is also not determined by foreground extinction.

The structure of the OMC-1 emission is of particular interest because this nebula is the best studied of the high-velocity sources in molecular clouds. Such sources frequently have bipolar structures, with more or less well-collimated streams of gas expanding from a central IR source (Bally and Lada 1983). Since we did not measure velocities, we cannot address specific problems of the outflow, but we have determined that the structure of the H_2 emission is not consistent with simple spherical geometry. The differences in emission across KL and weakness toward KL do roughly fit disk-constrained bipolar models such as that of Plambeck *et al.*

2. The increased extinction at the eastern and western edges of the source may be related to the dense quiescent molecular clouds Bastien *et al.* found there, but the levels of spatial detail in the two sets of observations are so different that it is difficult to determine the extent of the dense clouds' influence.

3. The $v = 3$–2 $S(3)$ line, combined with observations of other high-excitation transitions, indicates that there is a body of gas at $T \sim 2700$ K of column density $\sim 1.4 \times 10^{19}$ cm^{-2} on Pk 1, but no significant column of gas more than 3000 K.

This research was supported by NASA grant NSG-2412. S. V. B. acknowledges the support of the Alfred P. Sloan Foundation. We are grateful to E. E. Becklin, R. Koehler, C. Kaminsky, B. Shaffer, J. Clark, P. Foster, T. R. Geballe, A. Neal, and I. Y. Gatley for their assistance during the observing period, to Drs. D. Jennings and C. F. McKee for helpful discussions, and to an anonymous referee for comments. The instrument was built with a grant from the Research Corporation.

REFERENCES

Bally, J., and Lada, C. J. 1983, *Ap. J.*, **265**, 824.
Bastien, P., Bieging, J., Henkel, C., Martin, R. N., Pauls, T., Welmsky, C. M., Wilson, T. L., and Ziurys, L. M. 1981, *Astr. Ap.*, **98**, L4.
Beck, S. C. 1981, Ph.D. thesis, University of California at Berkeley.
Beck, S. C., Bloemhoff, E. E., Serabyn, E., Townes, C. H., Tokunaga, A. T., Lacy, J. H., and Smith, H. A. 1982, *Ap. J. (Letters)*, **253**, L83.
Beck, S. C., Lacy, J. H., and Geballe, T. R. 1979, *Ap. J. (Letters)*, **234**, L213.
Beckwith, S., Evans, N. J., II, Gatley, I., Gull, G., and Russell, R. W. 1983, *Ap. J.*, **264**, 152.
Beckwith, S., Persson, S. E., and Neugebauer, G. 1979, *Ap. J.*, **227**, 436.
Beckwith, S., Persson, S. E., Neugebauer, G., and Becklin, E. E. 1978, *Ap. J.*, **223**, 464.
Bragg, S. L., Brault, J. W., and Smith, W. H. 1982, *Ap. J.*, **263**, 999.
Davis, D. S., Larson, H. P., and Smith, H. A. 1982, *Ap. J.*, **259**, 166.
Downes, D., Genzel, R., Becklin, E. E., and Wynn-Williams, C. G. 1981, *Ap. J.*, **244**, 869.
Erickson, N., Goldsmith, P., Ulich, B., Lada, C., Beeson, R., Snell, R., and Huguenin, G. R. 1982, *Bull. AAS*, **14**, 627.
Johnson, H. L. 1968, in *Stars and Stellar Systems*, Vol. **7**, *Nebulae and Interstellar Matter*, ed. B. M. Middlehurst and L. H. Aller (Chicago: University of Chicago Press), p. 167.
Knacke, R. F., and Young, E. T. 1981, *Ap. J. (Letters)*, **249**, L65.
Nadeau, D., Geballe, T. R., and Neugebauer, G. 1982, *Ap. J.*, **253**, 154 (NGN).
Norman, C., and Silk, J. 1980, *Ap. J.*, **238**, 158.
Plambeck, R. L., Wright, M. C. H., Welch, W. J., Bieging, J. H., Baud, B., Ho, P. T. P., and Vogel, S. N. 1982, *Ap. J.*, **259**, 617.
Scoville, N. Z., Hall, D. N. B., Kleinmann, S. G., and Ridgeway, S. T. 1982, *Ap. J.*, **253**, 136.
Shull, J. M., and Beckwith, S. 1982, *Ann. Rev. Astr. Ap.*, **20**, 163.
Simon, M., Righini-Cohen, G., Joyce, R. R., and Simon, T. 1979, *Ap. J. (Letters)*, **230**, L175.
Thronson, H. A. 1981, *Ap. J.*, **248**, 984.
Turner, J., Kirby-Docken, K., and Dalgarno, A. 1977, *Ap. J. Suppl.*, **35**, 281.

S. C. Beck and S. Beckwith: Department of Astronomy, Cornell University, Ithaca, NY 14853-0352